Environmentally relevant perinatal exposure to DBP accelerated spermatogenesis by promoting the glycolipid metabolism of Sertoli cells in male mice

Tan Ma
Nanjing University
Yunhui Xia
Nanjing University
Bo Wang
Youjiang Medical University for Nationalities
Fenglian Yang
Youjiang Medical University for Nationalities
Jie Ding
Nanjing University
Jiang Wu
Nanjing University
Xiaodong Han
Nanjing University
Junli Wang
Youjiang Medical University for Nationalities
Dongmei Li (lidm@nju.edu.cn)
Nanjing University

Research Article

Keywords: Dibutyl phthalate, Monobutyl phthalate, Sertoli cells, Spermatogenesis, glycolipid metabolism

Posted Date: July 12th, 2022

DOI: https://doi.org/10.21203/rs.3.rs-1806257/v1

Abstract

Since Sertoli cells (SCs) play an important role in providing energy for spermatogenesis, the present study was aimed to investigate the effects of maternal exposure to plasticizer Dibutyl phthalate (DBP) on onset of spermatogenesis in male offspring through metabolism pathway as well as the underlying molecular mechanism. By detecting the level of the glucose metabolism in SCs, we found that monobutyl phthalate (MBP, the active metabolite of DBP) promoted cellular glycolysis accompanied by GLUT1, GLUT3, LDHA and MCT4 upregulated, leading to increased lactate which was provided spermatogenesis as energy substrate. Further mechanism research revealed that DBP/MBP increased fatty acid uptake and ATP production by promoting the expression of CD36, so as to accelerate their own maturity. Therefore, our findings provided new perspective at glycolipid metabolism to explain prenatal DBP exposure leading to earlier onset of spermatogenesis in male offspring mice.

1. Introduction

Dibutyl phthalate (DBP) is an endocrine-disrupting chemical that has the potential to cause adverse effects on male reproduction and development (Kavlock et al. 2002). As a typical plasticizer, DBP was widely used in cosmetics, children's toys, food packaging and medical devices to increase the flexibility of plastics (Kavlock et al. 2002; Pan et al. 2006). Due to the relatively weak interactions between DBP and plastics through hydrogen bonding or van der Waals's forces, DBP has been widely detected in the environment (Heudorf et al. 2007; Lottrup et al. 2006; Swan 2008). In some areas, the concentration of DBP in the environment has reached a hazardous level. For example, DBP levels of up to 55.7 mg/kg have been detected in South Xinjiang (Lü et al. 2018). Recent research found that the daily DBP exposure of residents in Beijing area was up to 81.8 μg/kg (Zhang et al. 2020). Furthermore, in some occasions, such as workers in the plastics manufacturing industry and infusion patients, DBP exposure can be as high as 10–20 mg/kg/day (Hauser et al. 2004; Koch et al. 2012; Rael et al. 2009; Seckin et al. 2009). In addition, DBP can be detected in pregnant women's serum, urine, amniotic fluid, and fetal cord blood, indicating that DBP can cross the placental barrier (Lien et al. 2015; Watkins et al. 2016). Our previous study has been found that maternal exposure to 50 mg/kg/day DBP induced earlier puberty and accelerated spermatogenesis (Ma et al. 2021), but the underlying molecular mechanism still needs to be further explored.

Spermatogenesis is an intricate process that results from multiple and complex interactions between various testicular cells (Alves et al. 2012). Sertoli cells (SCs) are mainly responsible for providing nutritional and structural support for the development of germ cells (Rato et al. 2012b; Svingen and Koopman 2013). The utilization of glucose in spermatogenesis is extremely limited, and the energy substrate is mainly lactate produced by SCs through glycolysis (Rato et al. 2012b). The glucose is transported into SCs by glucose transporters (GLUTs), and then is convert into pyruvate. Approximately 75% of pyruvate is catalyzed by lactate dehydrogenase (LDH) to produce lactate which is transported by monocarboxylic acid transporters (MCTs) to germ cell as energy metabolic substrate (Grootegoed et al. 1986; Oliveira et al. 2011; Rato et al. 2012a). Once the production of lactate secreted by SCs decrease, it

will disrupt the development of germ cells and affect male reproductive function (Rato et al. 2012a). However, it is not known whether DBP accelerates spermatogenesis by affecting glycolysis of SCs.

During spermatogenesis, approximately 75% of the developing spermatogenic cells will undergo physiological apoptosis (Huckins 1978; Johnson et al. 1983; Kubota and Brinster 2018; Oakberg 1956). In the final stage of spermatogenesis, the cytoplasm of the elongated spermatids are shed to form residual bodies (Kerr and de Kretser 1974). In this process, fatty acid (FA) transporter CD36 in SCs is transported from the cytoplasm to the plasma membrane to phagocytize apoptotic spermatogenic cells and residual bodies form lipid droplets (LDs), which is the key to maintaining the normal spermatogenesis (Chemes 1986; Gillot et al. 2005; Miething 1992; Pineau et al. 1991). Although glucose is a common substrate of energy, it is not the main metabolite used for ATP synthesis in SCs which require high energy levels for growth and functional normally (Riera et al. 2009). Xiong et al. report that SCs preferentially use lipids for β-oxidation as the main metabolic pathway for SCs to produce energy (Xiong et al. 2009). Our previous study showed that maternal exposure to 50 mg/kg/day DBP promotes juvenile SCs proliferation (Ma et al. 2020a). However, whether and how lipid metabolism is involved in DBP accelerating spermatogenesis are unclear.

In this study, from the perspective of maternal exposure of DBP to interfere with glucose and lipid metabolism in SCs, we studied the molecular mechanism of early spermatogenesis in male offspring. This provides a theoretical basis for explaining that environmental endocrine disruptors interfere with the onset of puberty by affecting SCs metabolism.

2. Methods

2.1. Animals and treatment

Nine-week-old male (n = 12) and female (n = 24) BALB/c mice (specific pathogen-free, SPF) were purchased from Qinglongshan animal breeding farm. Time-mated females that were observed to have a copulatory plug were considered to be at gestation day (GD) 0.5. After mating, pregnant females were randomized into four groups (n = 6 for each). Pregnant females were treated from GD 12.5 until birth with 0 (control), 50, 250, and 500 mg/kg/day DBP in 1 mL/kg corn oil administered daily by oral gavage. The 22-day-old males were euthanized by CO_2 asphyxiation. The testes were carefully removed for various examinations.

All experimental protocols were approved by the Animal Care and Use Committee of Nanjing University under the animal protocol number SYXK (Su) 2009-0017.

2.2. Reagents and cell culture

Fetal bovine serum (FBS), Triton® X-100, DMEM-F12 and MBP were purchased from Sigma-Aldrich Inc. (St. Louis, MO, USA). MBP (2.2224 g) was dissolved in 1 mL of DMSO to prepare a stock solution (10 M). The antibodies used in this study are listed in Table S1. TM4 cells were cultured in DMEM/F12 containing

10% FBS and 1% penicillinstreptomycin with a 5% CO_2 atmosphere in a humidified incubator at 37°C. TM4 cell lines were obtained from the American Type Culture Collection (Manassas, VA, USA). Primary SCs were prepared from three-week-old mice, as described previously (Ma et al. 2020b). Cells in the supernatant were collected and cultured (in DMEM-F12 medium containing 10% FBS) overnight. SCs that adhere to the bottom are obtained and irregularly shaped, while GCs are not attached and can be easily collected for inducing spontaneous apoptosis by culturing for 2 days based on a previous description (Xiong et al. 2009). Two days thereafter, cultures were subjected to a hypotonic treatment with 20 mM Tris (pH 7.4) for 3 min to lyse residual GCs. SCs were washed twice with PBS and then incubated in DMEM-F12.

2.3. Oligonucleotide Transfection

The small interfering RNA (siRNA) sequences used in this study were designed and chemically synthesized by HippoBio as: si-1 (sense: 5'-GCCAAGCUAUUGCGACAUGAUdTdT-3'; antisense: 5'-AUCAUGUCGCAAUAGCUUGGCdTdT-3'); si-2 (sense: 5'-GGAUCUGAAAUCGACCUUAAAdTdT-3'; antisense: 5'-UUUAAGGUCGAUUUCAGAUCCdTdT-3'); si-3 (sense: 5'- GCAGGUCAACAUAUUGGUCAAdTdT-3'; antisense: 5'- UUGACCAAUAUGUUGACCUGCdTdT-3'). Transfection was performed using Lipofectamine 2000 (Invitrogen) according to manufacturer's instructions.

2.4. Quantitative real-time PCR (qRT-PCR)

Analyses of qRT-PCR were performed as previously described (Chen et al. 2016). Total RNAs from cells or tissues were extracted using Trizol regent (Invitrogen, Carlsbad, CA. USA) and 1 μg mRNA was then reversed to cDNA using 5x HiScript Q RT SuperMix (Vazyme, Nanjing, China). Oligonucleotide primer sequences were listed in Table S2 and Glyceraldehyde-3-phosphate dehydrogenase (GAPDH) as an internal control. All analyses were performed using the $2^{-\Delta\Delta CT}$ method.

2.5. Western blotting

Western blotting analyses were executed as previously described (Chen et al. 2017). Specific antibody immunological complexes such as PPARγ, CD36, GLUT1, GLUT3, MCT4, LDHA, β-catenin, and GAPDH, were observed by enhanced chemiluminescence.

2.6. Immunofluorescent Staining

Immunofluorescence analyses of testis tissues or TM4 cells were performed as previously reported (Chen et al. 2016). The following primary antibodies were employed: mouse anti-CD36, mouse anti-Vimentin, mouse anti-GLUT1, rabbit anti-LDHA, rabbit anti-GLUT3, rabbit anti-SOX9, mouse anti-MCT4. The samples were subsequently treated with primary antibodies incubated at 4℃ overnight, followed by incubation of fluorophore-labelled secondary antibodies (Invitrogen) for 1 h at 37℃. The images were acquired by confocal fluorescence microscope (Olympus, Tokyo, Japan).

2.7. Lipid uptake assay

The free FAs uptake measurement kit (ab176768; Abcam) was used to measure FAs uptake in accordance with the manufacturer's protocol. In short, cells were seeded in a 96-well plate at a density of 50,000 cells per well 1 day before the measurement, and these cells were deprived of serum for 1 hour. Next, cells were incubated with TF2-C12 FAs at room temperature, and fluorescence (excitation: 485 nm, emission: 515 nm) was measured using a multifunctional fluorescence microplate reader (Molecular Devices, USA).

2.8. Triglycerides (TG) measurement

TG content was measured by TG detection kit (Jianchen, Nanjing). Briefly, cells cultured in 6-well plates were washed twice with phosphate-buffered saline (PBS) at room temperature. SCs were harvested by treated with 0.05% trypsin. Cells collected by centrifugation at 1000 rpm for 10 min were resuspended in PBS pH 7.4 and homogenized by ultrasonic irradiation. TG was measured by a routinely used method based on the colorimetric determination of the glycerol released upon the action of lipoproteinlipase on the TG. Results were expressed as millimoles TG/grams protein.

2.9. Glucose consumption evaluation

Glucose consumption by TM4 cells was measured by glucose detection kit (robio, Shanghai) according to the manufacturer's protocol.

2.10. Lactate determination

Lactate detection kit (Cablebridge Biotechnology, Shanghai) was purchased to examine lactate production in TM4 cells according to the manufacturer's protocol. Conditioned media obtained from cells cultured in 6-well plates were used to determine lactate production. Lactate was measured by a standard method involving the conversion of NAD + to NADH as described in Regueira et al (Regueira et al. 2014).

2.11. Cellular ATP measurement

The ATP levels in cells were detected using a commercial ATP assay kit (Beyotime Biotechnology) according to the protocol provided by the manufacturer. Briefly, after processing cells under different conditions, cells were lysed in lysis buffer, and centrifuged at 12000 g for 5 min at 4℃. The supernatant was used to detect the ATP level using a microplate reader (Beckman Coulter).

2.12. Flow cytometry

TM4 cells were processed for analysis of apoptosis and cell cycle using a FACScallbur flow cytometer (BD Biosciences). Cell apoptosis was analyzed by an Annexin V-FITC and PI staining kit (Vazyme, Nanjing, China) according to manufacturer’s instructions. For cell cycle analysis, cells were harvested and fixed in 70% (v/v) ethanol at 4℃ and then wash in PBS. All cells were stained with PI solution (50 μg/ml in PBS) (BD Biosciences) for 15 min in the dark, and the DNA content of each cell was detected by

FACScallbur flow cytometer (BD Biosciences). For cell surface staining, cells were harvested by trypsinization and washed in PBS. Cells were stained with anti-CD36-PE antibody for 30 min in PBS with 1% BSA and analyzed on FACScallbur flow cytometer (BD Biosciences).

2.13. Measurement of oxygen consumption rate and extracellular acidification rate

Cellular oxygen consumption rate (OCR) and extracellular acidification rate (ECAR) were used to monitor exogenous fatty acid oxidation (FAO) and glycolysis in real time when the appropriate substrates were added to or included in assay medium as indicated in the relevant experiments. Briefly, TM4 cells after indicated treatment were transferred on to XF microplates (5000 cells per well) in complete culture medium for 1 day. TM4 cells were washed and equilibrated for 1 hour. To determine FAO in TM4 cells, Mito Stress Tests were carried out using sequential injections of oligomycin (1 μM), FCCP (2 μM), and rotenone plus antimycin A (0.5 μM). To determine glycolysis in TM4 cells, glycolysis stress test was carried out using sequential injections of glucose (10 mM), oligomycin (1 μM), and 2-DG (50 mM). OCR and ECAR were recorded by an Extracellular Flux Analyzer XF96 (Seahorse Bioscience). Following each experiment, total cellular protein was determined using the Pierce BCA Protein Assay Kit (Vazyme, Nanjing, China).

2.14. LD staining

LDs in TM4 cells were stained with Nile Red. Nile Red staining of TM4 cells was performed as previously reported (Wang et al. 2015). Nuclei were stained with DAPI. Fluorescent signals were viewed by confocal fluorescence microscope (Olympus, Tokyo, Japan).

2.15. Statistical Analysis

The data were analyzed for statistical with SPSS 18.0 (SPSS, Chicago, IL, USA). The Student's t-test was used for paired comparisons; one-way ANOVA with Duncan's post hoc test was used to analyze the difference between groups. A *P* value of less than 0.05 was considered statistically significant.

3. Results

3.1. DBP/MBP promoted glucose metabolism in SCs

Our previous study has shown that maternal exposure to DBP accelerated spermatogenesis in offspring mice on PND 22 (Ma et al. 2021). Spermatogenesis is dependent on lactate which is supplied by SCs through glycolytic pathway. *In vivo*, we detected the expression of proteins (GLUT1, GLUT3, LDHA, and MCT4) that is involved in glycolysis by immunofluorescence. The results showed that the expression of

GLUT3, LDHA, and MCT4 increased at a dose of 50 mg/kg/day (Fig. 1A and Fig. S1). *In vitro*, compared with control group, lactate production increased significantly after exposure to 0.1 mM MBP (Fig. 1B). To further investigate the molecular mechanisms involved in lactate production, glucose uptake was analyzed. Results found that glucose uptake increased in TM4 cells exposed to 0.1 mM MBP compared with control group (Fig. 1C). Furthermore, 0.1 mM MBP obviously increased in glycolysis rate as well as total glycolytic capacity and reduced the mitochondrial respiratory capacity in TM4 cells (Fig. 1D and Fig. S2), as demonstrated by the changes in extracellular acidification rate (ECAR) and mitochondrial oxygen consumption rate (OCR), which might be maintaining redox balance for TM4 cells under toxic conditions. Consistent with the *in vivo* results, MBP increased the expression of GLUT1, GLUT3, LDHA, and MCT4 in the 0.1 mM group (Fig. 1E). A large number of studies have confirmed that β-catenin promotes glycolysis by regulating the expression of glycolysis related genes (Fan et al. 2018; Jiang et al. 2021). In this study, MBP increased the expression of β-catenin (Fig. 1E). Moreover, MBP also increased the expression of β-catenin both in the nuclei and cytoplasm of TM4 cells (Fig. 1F). The change in β-catenin expression was also confirmed by immunofluorescence (Fig. S3). Overall, the results suggested the increased glycolysis via β-catenin, the production and secretion of lactate, which may be one of the reasons for early spermatogenesis.

3.2. MBP promoted the increase of FAs in TM4 cells

In order to explore the effect of DBP on the lipid metabolism of SCs, we first detected the changes in FAs content in TM4 cells after MBP exposed. It was found that lipid droplets (LDs) accumulating in SCs in cytoplasmic areas close to their nuclei. Furthermore, the LDs number was increased in TM4 cells after MBP exposed (Fig. 2A). Correspondingly, we also found that the TG content of TM4 cells increased after MBP treatment (Fig. 2B). FAs are usually in the form of LDs after participating in the synthesis of TG (Gorga et al. 2017). Furthermore, we used qRT-PCR to detect the expression of genes involved in the synthesis and storage of TG in cells, and found that 0.1 mM MBP promoted the expression of Plin2, Gpat3, Gpat4, and Dgat1, but had no significant effect on Plin1, Plin3, Gpat1, and Gpat2 (Fig. 2C). Peroxisome proliferator-activated receptor γ (PPAR γ), as a ligand-activated transcription factor, affects lipid storage in SCs by regulating the expression of genes involved in fatty acid storage, such as the CD36, Plins, Dgat1, and Gpats (Gorga et al. 2017). In the present study, MBP induced marked enrichment of PPAR γ in the nuclei of TM4 cells (Fig. 2D). Overall, this result suggested that MBP promoted lipid storage of SCs by activating PPAR γ.

3.3. MBP promoted FA β-oxidation in TM4 cells

To determine whether MBP regulated FA β-oxidation, we first analyzed the expression of genes involved in FA β-oxidation in SCs following MBP treatment. As shown in Fig. 3A, most of the genes involved in FA β-oxidation were significantly upregulated in SCs treated with MBP as compared with control group. Furthermore, the basal and maximal oxygen consumption rates were significantly increased in TM4 cells after treatment with 0.1 mM MBP, indicating MBP promotes high level of FAs oxidation (Fig. 3B). Finally, to further determine the relationship between lipid oxidation and ATP production, we measured the production of ATP in TM4 cells after MBP exposed. The data showed that the production of ATP was

increased in 0.1 mM MBP-treated group (Fig. 3C). Taken together, these findings confirmed our hypothesis that accumulated lipid induced by DBP/MBP promoted FA oxidation to generate more energy for TM4 cells.

3.4. MBP promoted the uptake of exogenous FAs in TM4 cells

The sources of FAs in mammalian cells are mainly composed of the synthesis of intracellular FAs and the uptake of exogenous FAs (Kamphorst et al. 2013). Therefore, to explore the reasons for the increase of FAs, we measured gene levels of Fasn and Acaca, key components of the *de novo* FA biosynthesis. The result showed that the expression of Fasn was inhibited in TM4 cells after exposed to 0.1 mM MBP, whereas no changes of Acaca (Fig. 4A). Then, we measured gene levels of FATP1, FATP3, FATP4, and CD36, key components of the FA uptake. The qRT-PCR results showed that the expression of FATP1, FATP2, FATP3, and CD36 were increased compared with control, and the increased level of CD36 was the most significant (Fig. 4B). Furthermore, MBP treatment of TM4 cells showed markedly higher uptake of FAs than control group (Fig. 4C). These results suggested that an increased uptake of lipids might be a reason for the increased lipid accumulation in TM4 cells.

3.5. DBP/MBP promoted CD36 expression in SCs

As the above results found that the gene level of CD36 was the most significantly increased in TM4 cells after MBP-treated. Consist with *in vitro*, we also found that prenatal exposure to DBP (50 mg/kg/day) increased the levels of CD36 in the mouse testes, as shown by qRT-PCR assay (Fig. 5A). These results were further confirmed by Western blot and immunofluorescence (Fig. 5B and 5C). Because CD36 acts at the cell surface, we confirmed that plasma membrane localization of CD36 in TM4 cells after exposure to 0.1 mM MBP was enhanced by immunofluorescence (Fig. 5D and 5E). These results were further confirmed by flow cytometry (Fig. 5F).

3.6. CD36 increased in SCs co-cultured with apoptotic spermatogenic cells

Efficient phagocytic clearance of apoptotic spermatogenic cells by SCs is crucial for functional mature spermatogenesis (Dong et al. 2015). Previous study has confirmed that CD36 plays a key role in phagocytosis of germ cells, for constant production of mature spermatozoa (Gillot et al. 2005). In this study, we incubated primary cultured SCs with apoptotic germ cells. The gene and protein analyses revealed a time-dependent increase in the CD36 expression in the SCs co-cultured with apoptotic GCs (Fig. 6A and 6B), which indicating the potential involvement of CD36 in testicular phagocytosis. To determine whether the lipids result from engulfment of apoptotic germ cells, we examined the TG contents during co-culture of SCs with apoptotic germ cells. The results showed that the TG contents in SCs increased dramatically at 12 h (Fig. 6C). Long-chain acyl-CoA dehydrogenase (LCAD) is a key enzyme that catabolizes LCFAs in the β-oxidation pathway (Xiong et al. 2009). qRT-PCR analyses

revealed a time-dependent increase in the LCAD expression in the SCs co-cultured with apoptotic germ cells (Fig. 6D).

3.7. CD36 affected TM4 cells growth by promoting the uptake of exogenous FAs

To further confirm that CD36 facilitates FAs uptake, we examined whether blocking its expression by using small interfering RNA (siRNA) would abolish the FAs uptake in TM4 cells. qRT-PCR analysis demonstrated that siCD36-1 was more effective in suppressing the expression of CD36 (Fig. S4), and it was therefore selected for further studies. Function of CD36 as a lipid transporter was confirmed by CD36 siRNA knockdown, which attenuated lipid droplet accumulation (Fig. 7A). In addition, we determined TG content of TM4 cells with CD36 knockdown. Consistent with the above results, TG content was dampened in TM4 cells with CD36 knockdown as compared with control group (Fig. 7B). Furthermore, knockdown CD36 reduced the lipid uptake capacity in TM4 cells (Fig. 7C). These results suggested that lipid uptake and accumulation in TM4 cells were mediated via CD36. Previous study has demonstrated that SCs preferentially use the accumulated lipids as the source of fuels to produce energy for their growth (Xiong et al. 2009). Therefore, we analyzed the changes of ATP production and growth after knockdown of CD36 in TM4 cells. The data showed that ATP production was significantly attenuated in cells with CD36 knockdown (Fig. 7D). In addition, the results of flow cytometry showed that cells with CD36 knockdown increased apoptosis and decreased proliferation (Fig. 7E and 7F). We also measured the mitochondrial oxygen consumption rates (OCR) after knockdown of CD36 in TM4 cells. As shown in Fig. S5, CD36 knockdown showed an attenuated ATP production, markedly reduced maximal respiration and reserve capacity compared with control group. Taken together, these data confirmed that high levels of lipids uptake by CD36 mediated by DBP/MBP promoted to generate more energy and affected the growth of SCs.

4. Discussion

SCs perform a range of functions from physical support and immunoprotecting to the supplying of nutrients and other factors in order to achieve successful spermatogenesis (Oliveira et al. 2009; Rato et al. 2010). In addition, because of fixed number of germ cells supported by SCs, the proliferative capability of immature SCs before puberty determines the number of mature SC, the size of the testis, and the output of germ cells in the mature testis (Cheng et al. 2010). Our previous study found that maternal exposure to DBP promoted the formation of testicular TJs, which provided physical support for spermatogenesis (Ma et al. 2020b). In this study, we first found that DBP exposure could promote glycolipid metabolism in SCs, on this basis, we explored the mechanism of maternal exposure to DBP promoting the development of spermatogenic cells from the perspective of SCs metabolism.

As ‘nurse cells’, SCs are responsible for providing energy substrate lactate to developing germ cells. Modulation of metabolic pathways in SCs is likely to be determined by multiple elements including metabolic substrate availability and the action of hormones as well as other endogenous or exogenous

factors that will have a synergistic contribution to the progression of spermatogenesis (Rato et al. 2012b). Although Wang Zhang and his colleagues report that DBP exposure could induce liver lipid metabolism disorder and other hepatic toxicity through PPARα/SREBP-1c/FAS/GPAT/AMPK signal pathway (Zhang et al. 2021), there are still few studies on the effect of DBP on cell metabolism.

Developing germ cells have specific metabolic requirements, and the lactate produced by SCs through glycolysis is preferentially used as a substrate for ATP production (Robinson and Fritz 1981). SCs produce lactate primarily from glucose, and the rate-limiting step is the membrane passage of glucose from the extracellular space, via specific GLUTs (Angulo et al. 1998). Three GLUTs (GLUT1, GLUT3 and GLUT8) have been identified in SCs to date (Carosa et al. 2005; Galardo et al. 2008). However, GLUT8 is not expected to be involved in glucose transport from the extracellular (Piroli et al. 2002). In this study, we found that MBP promoted GLUT1 and GLUT3 expression in SCs, which was consistent with MBP promoting glucose uptake in SCs. LDH has a crucial role in providing lactate to developing germ cells, and LDHA is the predominantly expressed isoform in the testes(Hawtrey and Goldberg 1968). The export of lactate from SCs by MCTs is responsible for lactate supply to germ cells (Oliveira et al. 2011; Rato et al. 2012a). A total of 14 MCT family members have been identified in tissues and cells, among which MCT1 and MCT4 are expressed in SCs (Bonen et al. 2006; Galardo et al. 2007). MCT1 has a high affinity for lactate and is mainly responsible for the uptake of lactate from the extracelluar environment into cell (Bonen 2001), while MCT4 has a low affinity for lactate and is mainly responsible for export of lactate into the extra-Sertoli cellular space (Bonen 2001; Galardo et al. 2007). Our study found that MBP promoted the expression of LDHA and MCT4, indicating that MBP promoted the synthesis and secretion of lactate in SCs. Furthermore, 0.1mM MBP decreased OCR and increased ECAR in SCs by Seahorse analysis, confirming the increase in glycolysis of SCs. Therefore, MBP promotes the synthesis and secretion of lactate in SCs, which might to provide energy support for the early initiation of spermatogenesis.

The presence of numerous LDs is characteristic in mature SCs and these LDs are assumed to constitute the storage of FAs. Previous study showed that the inactivation of lipid metabolism-related genes in mice could impair spermatogenesis, indicating that lipid metabolism is essential for male reproduction (Gorga et al. 2017). SCs devour residual body and apoptotic germ cells, resulting in an increase of the lipid contents in SCs (Oliveira et al. 2015). Xiong and collaborators show that SCs preferentially use lipid as an energy source (Xiong et al. 2009). In our study, we found that MBP increased the content of TG and promoted lipid metabolism in SCs, which was not dependent on the *de novo* synthesis in SCs, but on the increased uptake of external FAs. CD36 has high affinity for FAs and facilitates tissue FA uptake in rodents and humans (Glatz et al. 2010; Hames et al. 2014). With increasing CD36 expression, we found that the uptake of FAs, the TG content, and the ATP production was increased. Furthermore, we showed that CD36 knockdown resulted in decreased ATP production and increased apoptosis in SCs. Therefore, we found that MBP enhanced lipid metabolism and ATP production by promoting the expression of CD36.

5. Conclusions

In summary, we first confirmed that DBP/MBP increased the production of lactate via glycolysis through the expression of the key glycolytic-related proteins GLUT1, GLUT3, LDHA and MCT4, and promoted lipid metabolism in SCs at a relatively low concentration range, which might accelerate the spermatogenesis during puberty. Then, we found that CD36 played an important role in DBP/MBP exposure resulting in increased lipid uptake and ATP production as well as promoting survival of SCs (Fig. 8). Therefore, our findings are the first explain the reason why prenatal DBP exposure leads to early spermatogenesis in male offspring mice from the perspective of metabolism.

Declarations

Author contribution

Tan Ma, Yunhui Xia, and Jie Ding has full access to all data in the study and are responsible for the integrity of the data and the accuracy of data analysis. Junli Wang and Dongmei Li contributed to the research design, conducted experiments, assisted the analysis of samples, and participated in the interpretation of the results and the writing of the manuscript. Jiang Wu, Bo Wang, Fenglian Yang and Xiaodong Han participated in the discussion of the results.

Funding

This work was supported by National Natural Science Foundation of China (31971517, 31870492 and 82060293) and Foundation of Central Government to Guide Local Scientific and Technological Development (No. ZY21195023)

Data availability

All the data in this study are available from the corresponding author upon reasonable request.

Code availability

Not applicable.

Ethics approval

All experimental protocols were approved by the Animal Care and Use Committee of Nanjing University under the animal protocol number SYXK (Su) 2009-0017.

Consent for publication

No personal information is included in this study.

Conflict of interest

The authors report no conflicts of interest.

References

1. Alves MG, Rato L, Carvalho RA, Moreira PI, Socorro S, Oliveira PF. 2012. Hormonal control of sertoli cell metabolism regulates spermatogenesis. Cellular and Molecular Life Sciences 70:777–793.
2. Angulo C, Rauch MC, Droppelmann A, Reyes AM, Slebe JC, Delgado-López F, et al. 1998. Hexose transporter expression and function in mammalian spermatozoa: Cellular localization and transport of hexoses and vitamin c. Journal of cellular biochemistry 71:189–203.
3. Bonen A. 2001. The expression of lactate transporters (mct1 and mct4) in heart and muscle. European journal of applied physiology 86:6–11.
4. Bonen A, Heynen M, Hatta H. 2006. Distribution of monocarboxylate transporters mct1-mct8 in rat tissues and human skeletal muscle. Applied physiology, nutrition, and metabolism = Physiologie appliquee, nutrition et metabolisme 31:31–39.
5. Carosa E, Radico C, Giansante N, Rossi S, D'Adamo F, Di Stasi SM, et al. 2005. Ontogenetic profile and thyroid hormone regulation of type-1 and type-8 glucose transporters in rat sertoli cells. International journal of andrology 28:99–106.
6. Chemes H. 1986. The phagocytic function of sertoli cells: A morphological, biochemical, and endocrinological study of lysosomes and acid phosphatase localization in the rat testis. Endocrinology 119:1673–1681.
7. Chen Y, Zhou Y, Wang J, Wang L, Xiang Z, Li D, et al. 2016. Microcystin-leucine arginine causes cytotoxic effects in sertoli cells resulting in reproductive dysfunction in male mice. Scientific reports 6:39238.
8. Chen Y, Wang J, Zhang Q, Xiang Z, Li D, Han X. 2017. Microcystin-leucine arginine exhibits immunomodulatory roles in testicular cells resulting in orchitis. Environmental pollution (Barking, Essex: 1987) 229:964–975.
9. Cheng CY, Wong EW, Yan HH, Mruk DD. 2010. Regulation of spermatogenesis in the microenvironment of the seminiferous epithelium: New insights and advances. Molecular and cellular endocrinology 315:49–56.
10. Dong Ys, Hou Wg, Li Y, Liu Db, Hao Gz, Zhang Hf, et al. 2015. Unexpected requirement for a binding partner of the syntaxin family in phagocytosis by murine testicular sertoli cells. Cell Death & Differentiation 23:787–800.
11. Fan Q, Yang L, Zhang X, Ma Y, Li Y, Dong L, et al. 2018. Autophagy promotes metastasis and glycolysis by upregulating mct1 expression and wnt/β-catenin signaling pathway activation in hepatocellular carcinoma cells. Journal of Experimental & Clinical Cancer Research 37.
12. Galardo MN, Riera MF, Pellizzari EH, Cigorraga SB, Meroni SB. 2007. The amp-activated protein kinase activator, 5-aminoimidazole-4-carboxamide-1-b-d-ribonucleoside, regulates lactate production in rat sertoli cells. Journal of molecular endocrinology 39:279–288.

13. Galardo MN, Riera MF, Pellizzari EH, Chemes HE, Venara MC, Cigorraga SB, et al. 2008. Regulation of expression of sertoli cell glucose transporters 1 and 3 by fsh, il1 beta, and bfgf at two different time-points in pubertal development. Cell and tissue research 334:295–304.
14. Gillot I, Jehl-Pietri C, Gounon P, Luquet S, Rassoulzadegan M, Grimaldi P, et al. 2005. Germ cells and fatty acids induce translocation of cd36 scavenger receptor to the plasma membrane of sertoli cells. Journal of cell science 118:3027–3035.
15. Glatz JF, Luiken JJ, Bonen A. 2010. Membrane fatty acid transporters as regulators of lipid metabolism: Implications for metabolic disease. Physiological reviews 90:367–417.
16. Gorga A, Rindone GM, Regueira M, Pellizzari EH, Camberos MC, Cigorraga SB, et al. 2017. Pparγ activation regulates lipid droplet formation and lactate production in rat sertoli cells. Cell and tissue research 369:611–624.
17. Grootegoed JA, Oonk RB, Jansen R, van der Molen HJ. 1986. Metabolism of radiolabelled energy-yielding substrates by rat sertoli cells. Journal of reproduction and fertility 77:109–118.
18. Hames KC, Vella A, Kemp BJ, Jensen MD. 2014. Free fatty acid uptake in humans with cd36 deficiency. Diabetes 63:3606–3614.
19. Hauser R, Duty S, Godfrey-Bailey L, Calafat AM. 2004. Medications as a source of human exposure to phthalates. Environmental health perspectives 112:751–753.
20. Hawtrey C, Goldberg E. 1968. Differential synthesis of ldh in mouse testes. Annals of the New York Academy of Sciences 151:611–615.
21. Heudorf U, Mersch-Sundermann V, Angerer J. 2007. Phthalates: Toxicology and exposure. International journal of hygiene and environmental health 210:623–634.
22. Huckins C. 1978. The morphology and kinetics of spermatogonial degeneration in normal adult rats: An analysis using a simplified classification of the germinal epithelium. The Anatomical record 190:905–926.
23. Jiang Y, Han Q, Zhao H, Zhang J. 2021. Promotion of epithelial-mesenchymal transformation by hepatocellular carcinoma-educated macrophages through wnt2b/β-catenin/c-myc signaling and reprogramming glycolysis. Journal of Experimental & Clinical Cancer Research 40.
24. Johnson L, Petty CS, Neaves WB. 1983. Further quantification of human spermatogenesis: Germ cell loss during postprophase of meiosis and its relationship to daily sperm production. Biology of reproduction 29:207–215.
25. Kamphorst JJ, Cross JR, Fan J, de Stanchina E, Mathew R, White EP, et al. 2013. Hypoxic and ras-transformed cells support growth by scavenging unsaturated fatty acids from lysophospholipids. Proceedings of the National Academy of Sciences of the United States of America 110:8882–8887.
26. Kavlock R, Boekelheide K, Chapin R, Cunningham M, Faustman E, Foster P, et al. 2002. Ntp center for the evaluation of risks to human reproduction: Phthalates expert panel report on the reproductive and developmental toxicity of di-n-butyl phthalate. Reproductive toxicology (Elmsford, NY) 16:489–527.
27. Kerr JB, de Kretser DM. 1974. Proceedings: The role of the sertoli cell in phagocytosis of the residual bodies of spermatids. Journal of reproduction and fertility 36:439–440.

28. Koch HM, Christensen KL, Harth V, Lorber M, Brüning T. 2012. Di-n-butyl phthalate (dnbp) and diisobutyl phthalate (dibp) metabolism in a human volunteer after single oral doses. Archives of toxicology 86:1829–1839.
29. Kubota H, Brinster RL. 2018. Spermatogonial stem cells. Biology of reproduction 99:52–74.
30. Lien YJ, Ku HY, Su PH, Chen SJ, Chen HY, Liao PC, et al. 2015. Prenatal exposure to phthalate esters and behavioral syndromes in children at 8 years of age: Taiwan maternal and infant cohort study. Environmental health perspectives 123:95–100.
31. Lottrup G, Andersson AM, Leffers H, Mortensen GK, Toppari J, Skakkebaek NE, et al. 2006. Possible impact of phthalates on infant reproductive health. International journal of andrology 29:172–180; discussion 181 – 175.
32. Lü H, Mo CH, Zhao HM, Xiang L, Katsoyiannis A, Li YW, et al. 2018. Soil contamination and sources of phthalates and its health risk in china: A review. Environmental research 164:417–429.
33. Ma T, Hou J, Zhou Y, Chen Y, Qiu J, Wu J, et al. 2020a. Dibutyl phthalate promotes juvenile sertoli cell proliferation by decreasing the levels of the e3 ubiquitin ligase pellino 2. Environmental health: a global access science source 19:87.
34. Ma T, Zhou Y, Xia Y, Meng X, Jin H, Wang B, et al. 2020b. Maternal exposure to di-n-butyl phthalate promotes the formation of testicular tight junctions through downregulation of nf-κb/cox-2/pge(2)/mmp-2 in mouse offspring. Environmental science & technology 54:8245–8258.
35. Ma T, Zhou Y, Xia Y, Jin H, Wang B, Wu J, et al. 2021. Environmentally relevant perinatal exposure to dbp disturbs testicular development and puberty onset in male mice. Toxicology 459:152860.
36. Miething A. 1992. Germ-cell death during prespermatogenesis in the testis of the golden hamster. Cell and tissue research 267:583–590.
37. Oakberg EF. 1956. A description of spermiogenesis in the mouse and its use in analysis of the cycle of the seminiferous epithelium and germ cell renewal. The American journal of anatomy 99:391–413.
38. Oliveira PF, Sousa M, Barros A, Moura T, Rebelo da Costa A. 2009. Membrane transporters and cytoplasmatic ph regulation on bovine sertoli cells. The Journal of membrane biology 227:49–55.
39. Oliveira PF, Alves MG, Rato L, Silva J, Sá R, Barros A, et al. 2011. Influence of 5α-dihydrotestosterone and 17β-estradiol on human sertoli cells metabolism. International journal of andrology 34:e612-620.
40. Oliveira PF, Martins AD, Moreira AC, Cheng CY, Alves MG. 2015. The warburg effect revisited–lesson from the sertoli cell. Medicinal research reviews 35:126–151.
41. Pan G, Hanaoka T, Yoshimura M, Zhang S, Wang P, Tsukino H, et al. 2006. Decreased serum free testosterone in workers exposed to high levels of di-n-butyl phthalate (dbp) and di-2-ethylhexyl phthalate (dehp): A cross-sectional study in china. Environmental health perspectives 114:1643–1648.
42. Pineau C, Le Magueresse B, Courtens JL, Jégou B. 1991. Study in vitro of the phagocytic function of sertoli cells in the rat. Cell and tissue research 264:589–598.

43. Piroli GG, Grillo CA, Hoskin EK, Znamensky V, Katz EB, Milner TA, et al. 2002. Peripheral glucose administration stimulates the translocation of glut8 glucose transporter to the endoplasmic reticulum in the rat hippocampus. The Journal of comparative neurology 452:103–114.
44. Rael LT, Bar-Or R, Ambruso DR, Mains CW, Slone DS, Craun ML, et al. 2009. Phthalate esters used as plasticizers in packed red blood cell storage bags may lead to progressive toxin exposure and the release of pro-inflammatory cytokines. Oxidative medicine and cellular longevity 2:166–171.
45. Rato L, Socorro S, Cavaco JE, Oliveira PF. 2010. Tubular fluid secretion in the seminiferous epithelium: Ion transporters and aquaporins in sertoli cells. The Journal of membrane biology 236:215–224.
46. Rato L, Alves MG, Socorro S, Carvalho RA, Cavaco JE, Oliveira PF. 2012a. Metabolic modulation induced by oestradiol and dht in immature rat sertoli cells cultured in vitro. Bioscience reports 32:61–69.
47. Rato L, Alves MG, Socorro S, Duarte AI, Cavaco JE, Oliveira PF. 2012b. Metabolic regulation is important for spermatogenesis. Nature reviews Urology 9:330–338.
48. Regueira M, Riera MF, Galardo MN, Pellizzari EH, Cigorraga SB, Meroni SB. 2014. Activation of ppar α and ppar β/δ regulates sertoli cell metabolism. Molecular and cellular endocrinology 382:271–281.
49. Riera MF, Galardo MN, Pellizzari EH, Meroni SB, Cigorraga SB. 2009. Molecular mechanisms involved in sertoli cell adaptation to glucose deprivation. American journal of physiology Endocrinology and metabolism 297:E907-914.
50. Robinson R, Fritz IB. 1981. Metabolism of glucose by sertoli cells in culture. Biology of reproduction 24:1032–1041.
51. Seckin E, Fromme H, Völkel W. 2009. Determination of total and free mono-n-butyl phthalate in human urine samples after medication of a di-n-butyl phthalate containing capsule. Toxicology letters 188:33–37.
52. Svingen T, Koopman P. 2013. Building the mammalian testis: Origins, differentiation, and assembly of the component cell populations. Genes & development 27:2409–2426.
53. Swan SH. 2008. Environmental phthalate exposure in relation to reproductive outcomes and other health endpoints in humans. Environmental research 108:177–184.
54. Wang W, Wei S, Li L, Su X, Du C, Li F, et al. 2015. Proteomic analysis of murine testes lipid droplets. Scientific reports 5:12070.
55. Watkins DJ, Peterson KE, Ferguson KK, Mercado-García A, Tamayo y Ortiz M, Cantoral A, et al. 2016. Relating phthalate and bpa exposure to metabolism in peripubescence: The role of exposure timing, sex, and puberty. The Journal of clinical endocrinology and metabolism 101:79–88.
56. Xiong W, Wang H, Wu H, Chen Y, Han D. 2009. Apoptotic spermatogenic cells can be energy sources for sertoli cells. Reproduction (Cambridge, England) 137:469–479.
57. Zhang W, Li JY, Wei XC, Wang Q, Yang JY, Hou H, et al. 2021. Effects of dibutyl phthalate on lipid metabolism in liver and hepatocytes based on pparα/srebp-1c/fas/gpat/ampk signal pathway. Food

and chemical toxicology: an international journal published for the British Industrial Biological Research Association 149:112029.

58. Zhang X, Tang S, Qiu T, Hu X, Lu Y, Du P, et al. 2020. Investigation of phthalate metabolites in urine and daily phthalate intakes among three age groups in beijing, china. Environmental pollution (Barking, Essex: 1987) 260:114005.

Figures

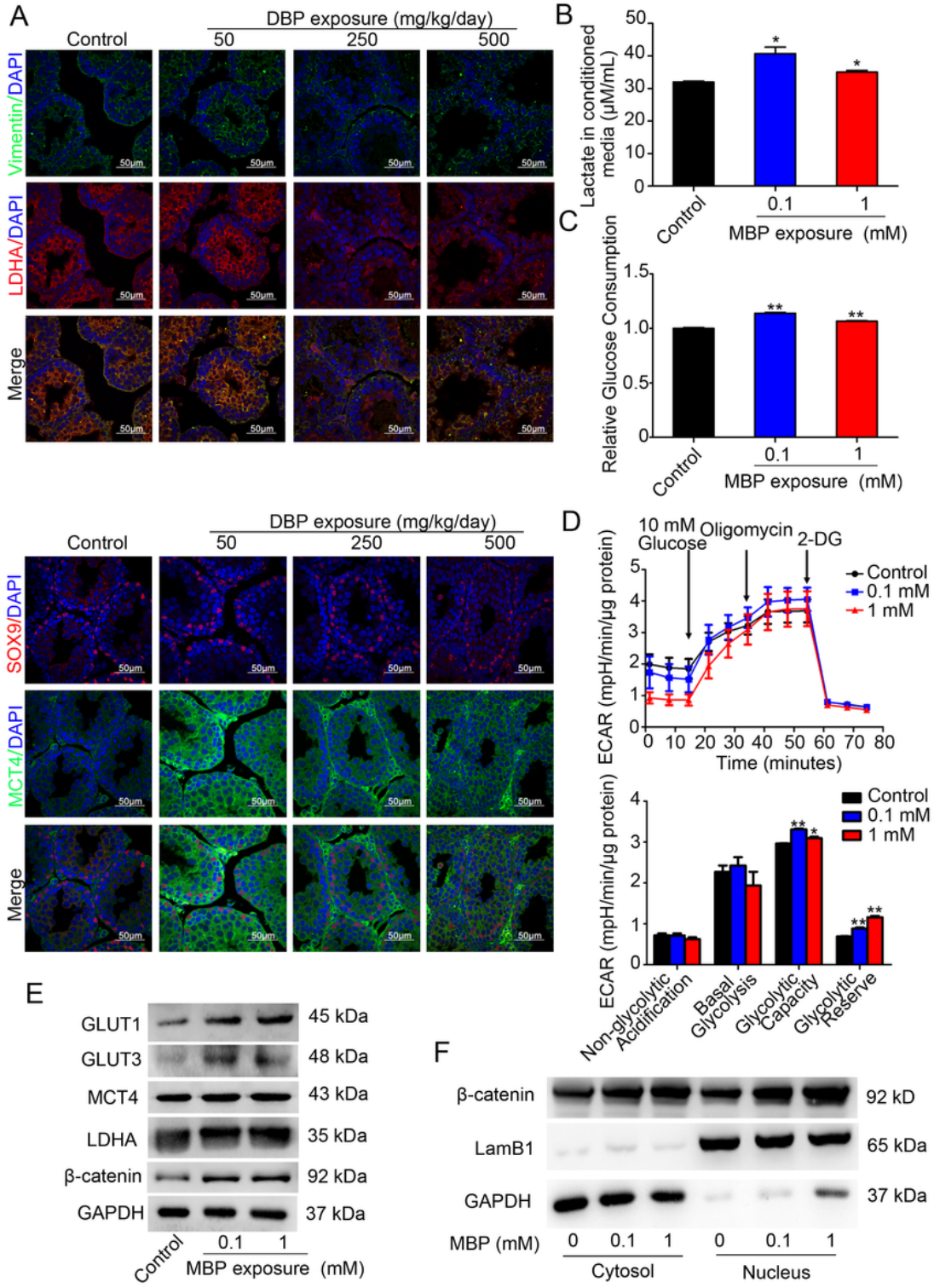

Figure 1

Effect of DBP/MBP on glucose metabolism in SCs. (A) Colocalization of Alexa Fluor 488-labeled MCT4 (green) with Alexa Fluor 594-labeled SOX9 (red, a marker of SCs), Alexa Fluor 594-labeled LDHA (red) with Alexa Fluor 488-labeled vimentin (green, a marker of SCs) in the testis was examined using a confocal fluorescence microscope. TM4 cells were treated with various concentration of MBP for 24 h. (B) Lactate production was determined using a commercial assay kit. (C) Glucose consumption was determined

using a commercial assay kit. (D) Extracellular acidification rates (ECAR) of Control and MBP-treated TM4 cells before or after indicated treatments. (E) The expression levels of proteins related to glucose metabolism were analyzed by Western blot. GAPDH was run as an internal control. (F) Nuclear and cytosolic fractions were prepared from the control and MBP-induced TM4 cells. Levels of β-catenin were analyzed by western blot. GAPDH and Lamin B1 served as cytosolic and nuclear markers, respectively. Results are expressed as means ± SEM (n = 3). ** $P < 0.01$; * $P < 0.05$, compared with the control.

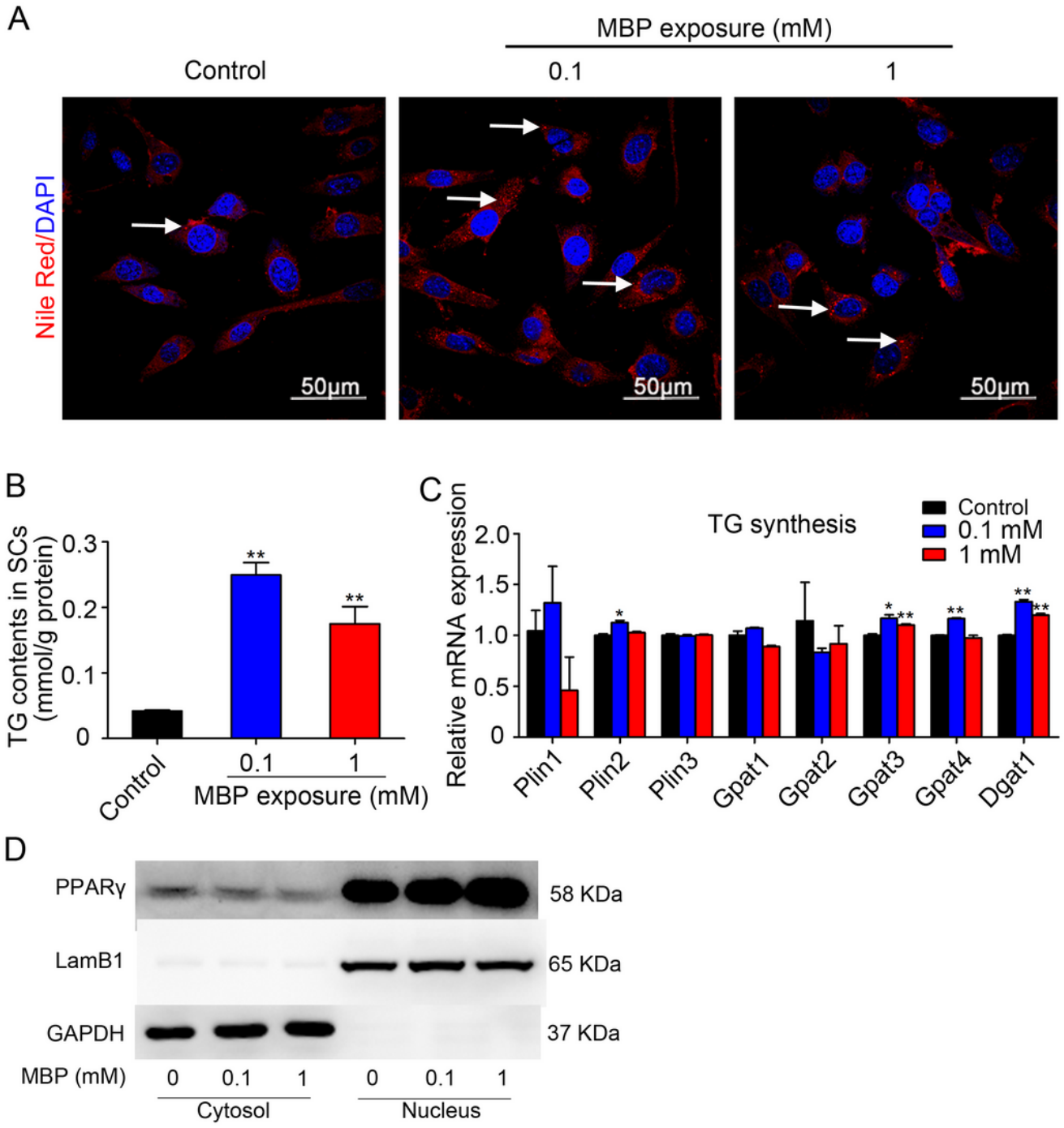

Figure 2

Effect of monobutyl phthalate (MBP) on triglycerides (TG) levels and lipid droplet (LD) formation in TM4 cells. TM4 cells were treated with various concentration of MBP for 24 h. (A) Intracellular lipid content visualized with nile red (red) staining. Nuclei were stained with DAPI (blue). The arrow indicates lipid droplet. (B) TG levels were determined in cell lysates and expressed as millimoles TG/grams protein. (C) Relative mRNA expression of genes related to fatty acid storage in TM4 cells. GAPDH was run as an internal control. (D) Nuclear and cytosolic fractions were prepared from the control and MBP-induced TM4 cells. Levels of PPARγ were analyzed by western blot. GAPDH and Lamin B1 served as cytosolic and nuclear markers, respectively. Results are expressed as means ± SEM (n = 3). ** $P < 0.01$; * $P < 0.05$, compared with the control.

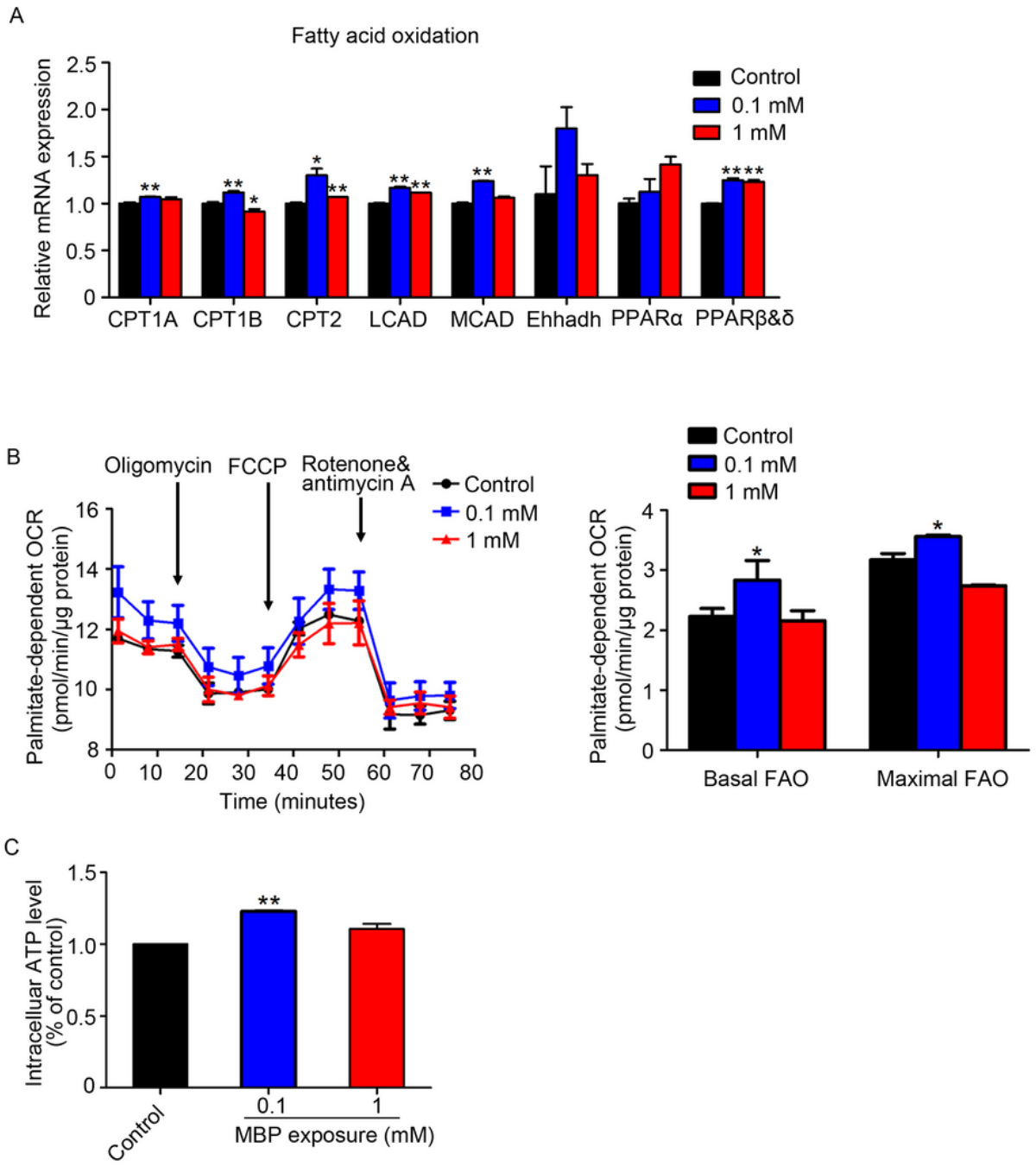

Figure 3

Effect of MBP on FAs oxidation in TM4 cells. TM4 cells were treated with various concentration of MBP for 24 h. (A) Relative mRNA expression of indicated genes related to lipid β-oxidation in TM4 cells. GAPDH was run as an internal control. (B) The oxygen consumption rate (OCR) was determined using Seahorse XF analyzers. (C) The intracellular ATP content was performed using an ATP Assay Kit by a

microbeta counter. Results are expressed as means ± SEM (n = 3). ** $P < 0.01$; * $P < 0.05$, compared with the control.

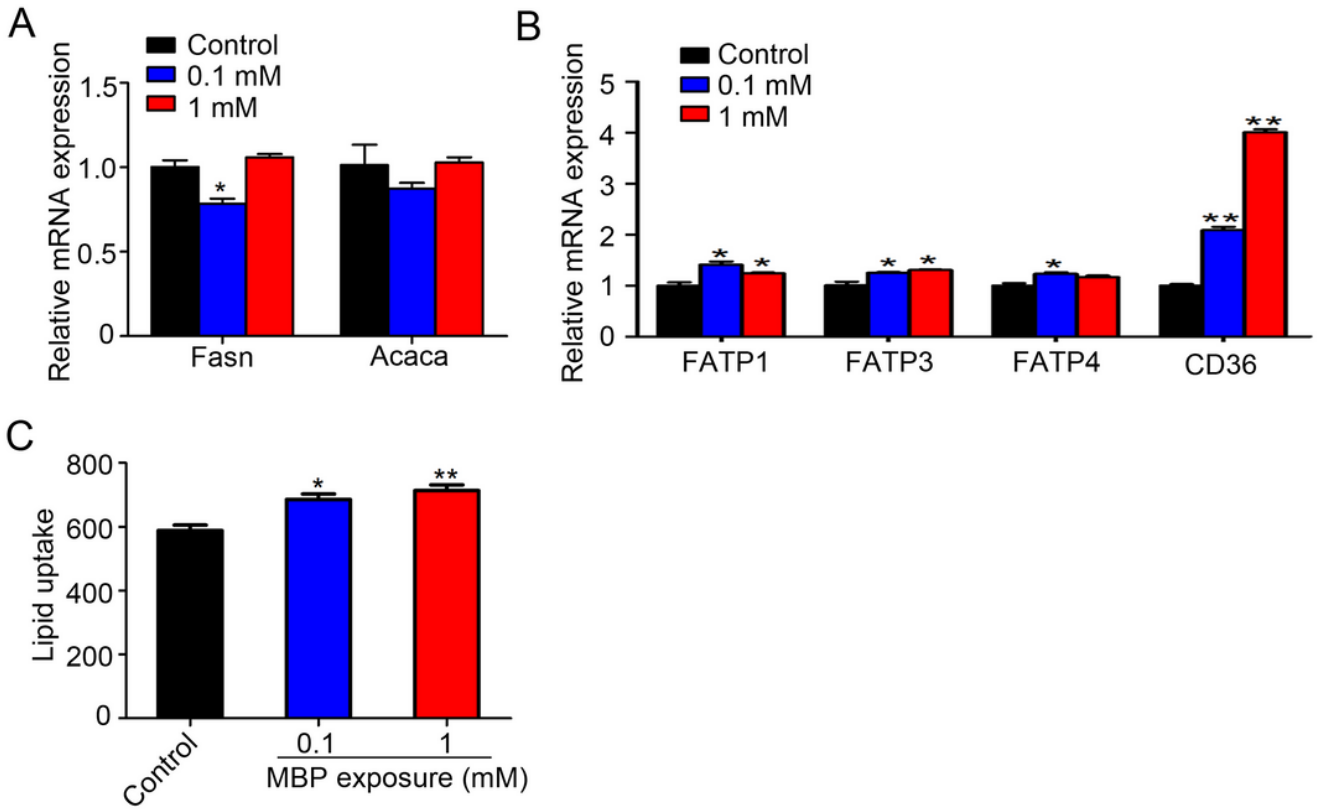

Figure 4

Effect of MBP on fatty acid uptake in TM4 cells. TM4 cells were treated with various concentration of MBP for 24 h. (A) Relative mRNA expression of genes related to *de novo* lipogenesis in TM4 cells. GAPDH was run as an internal control. (B) Relative mRNA expression of genes related to exogenous uptake of FAs in TM4 cells. GAPDH was run as an internal control. (C) Bar graph depicting ELISA results of fatty acid uptake by TM4 cells using a Free Fatty Acid Uptake Assay Kit. Results are expressed as means ± SEM (n = 3). ** $P < 0.01$; * $P < 0.05$, compared with the control.

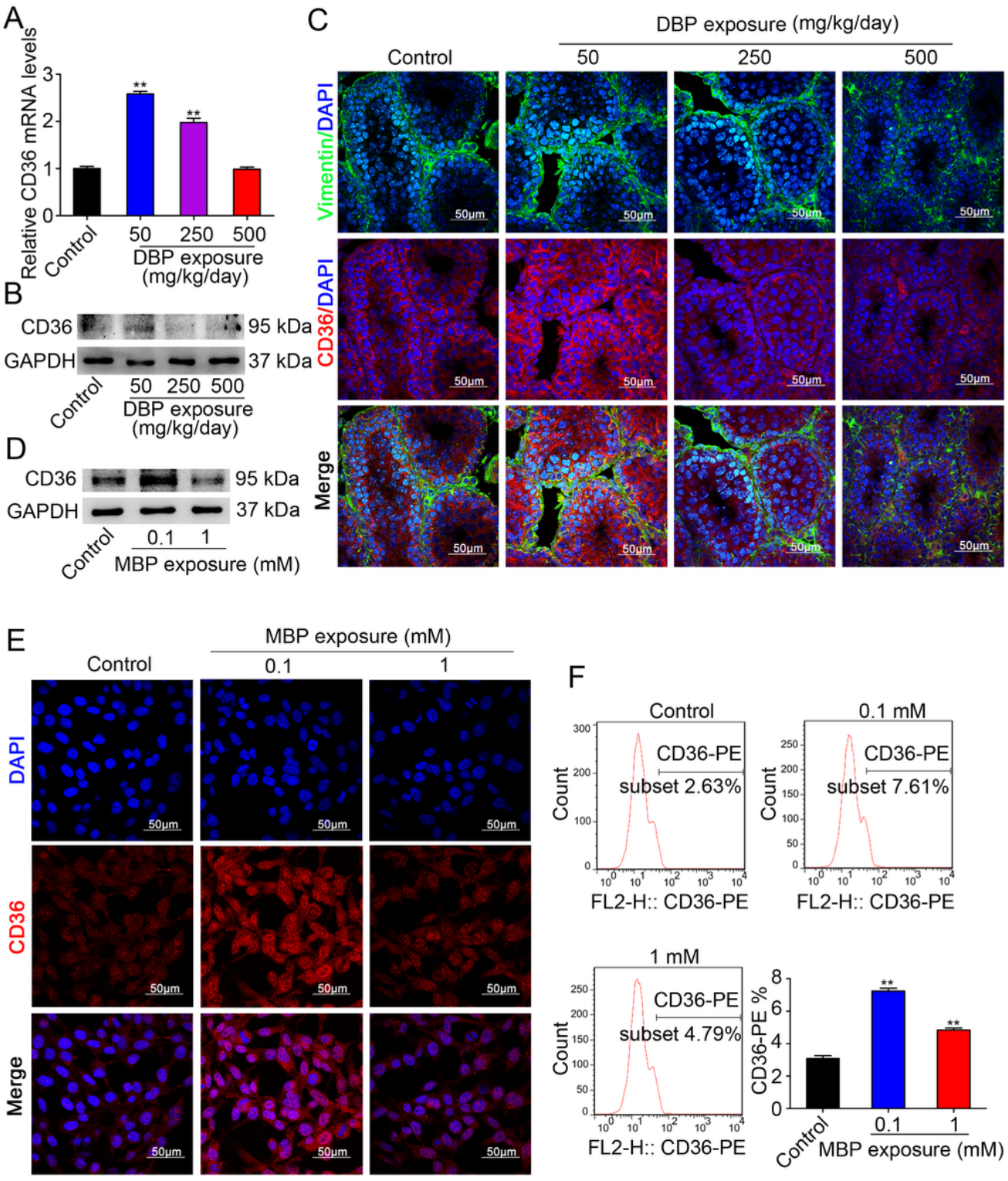

Figure 5

Effect of DBP/MBP on CD36 expression in SCs. (A) CD36 mRNA expression levels in testis were analyzed by qRT-PCR. GAPDH was run as an internal control (n = 3). (B) The expression levels of CD36 in testis were analyzed by Western blot. GAPDH was run as an internal control (n = 3). (C) Co-localization of Alexa Fluor 488-labeled Vimentin (green, a marker of SCs) with Alexa Fluor 594-labeled CD36 in testis was examined by a confocal fluorescence microscope. TM4 cells were treated with various concentration of

MBP for 24 h. (D) The expression levels of CD36 were analyzed by Western blot. GAPDH was run as an internal control (n = 3). (E) The expression levels of CD36 were analyzed by Immunofluorescence. (F) The expression levels of CD36 in cell surface were analyzed by Flow cytometry. Results are expressed as means ± SEM (n = 3). ** $P < 0.01$; * $P < 0.05$, compared with the control.

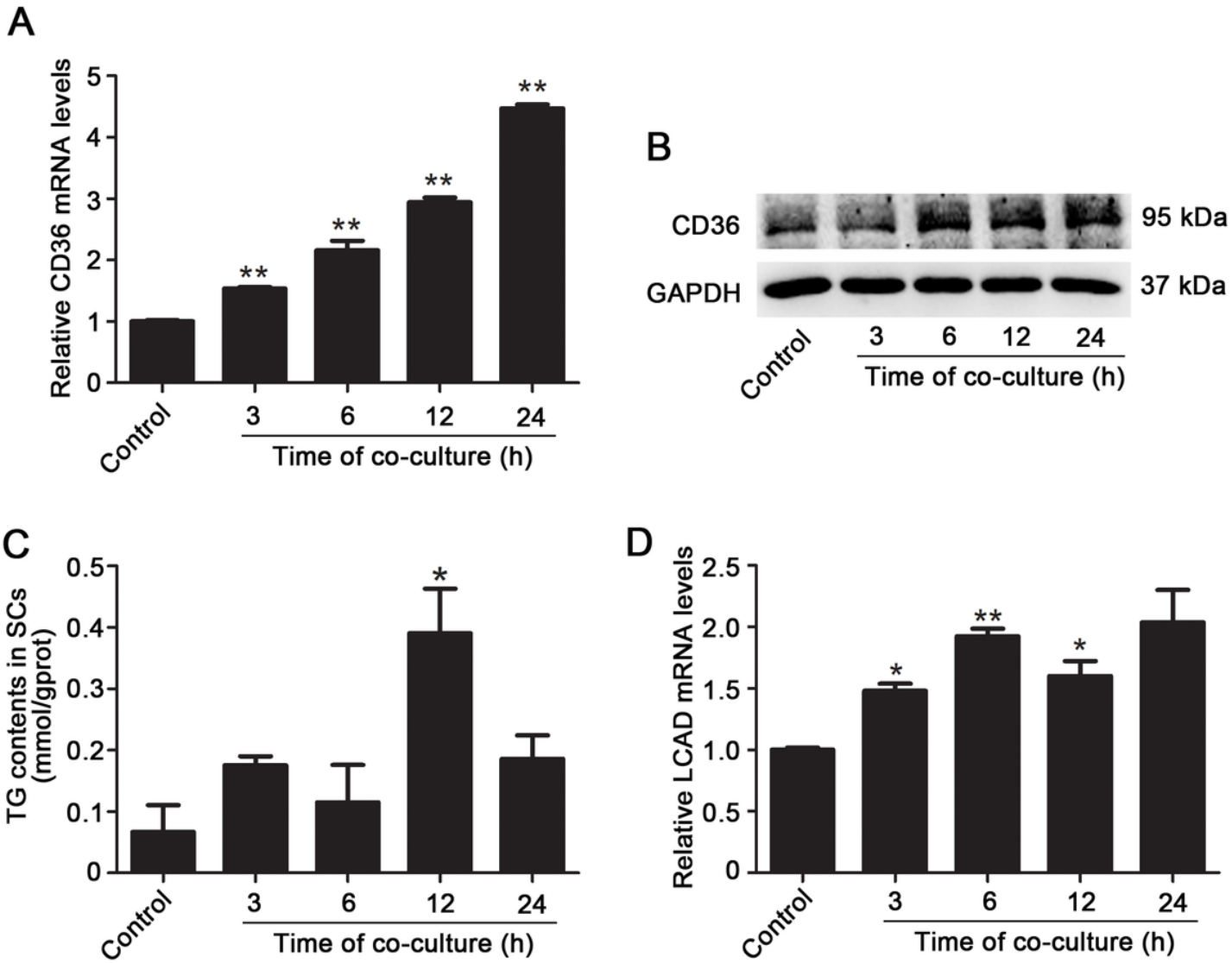

Figure 6

Effect of apoptotic germ cells on CD36 expression in SCs. Apoptotic germ cells co-culture with SCs at 0, 3, 6, 12, and 24 h. (A) CD36 mRNA expression levels in SCs were analyzed by qRT-PCR. GAPDH was run as an internal control. (B) The expression levels of CD36 in SCs were analyzed by Western blot. GAPDH was run as an internal control. (C) TG levels were determined in SCs lysates and expressed as millimoles TG/grams protein. (D) LCAD mRNA expression levels in SCs were analyzed by qRT-PCR. GAPDH was run as an internal control. Results are expressed as means ± SEM (n = 3). ** $P < 0.01$; * $P < 0.05$, compared with the control.

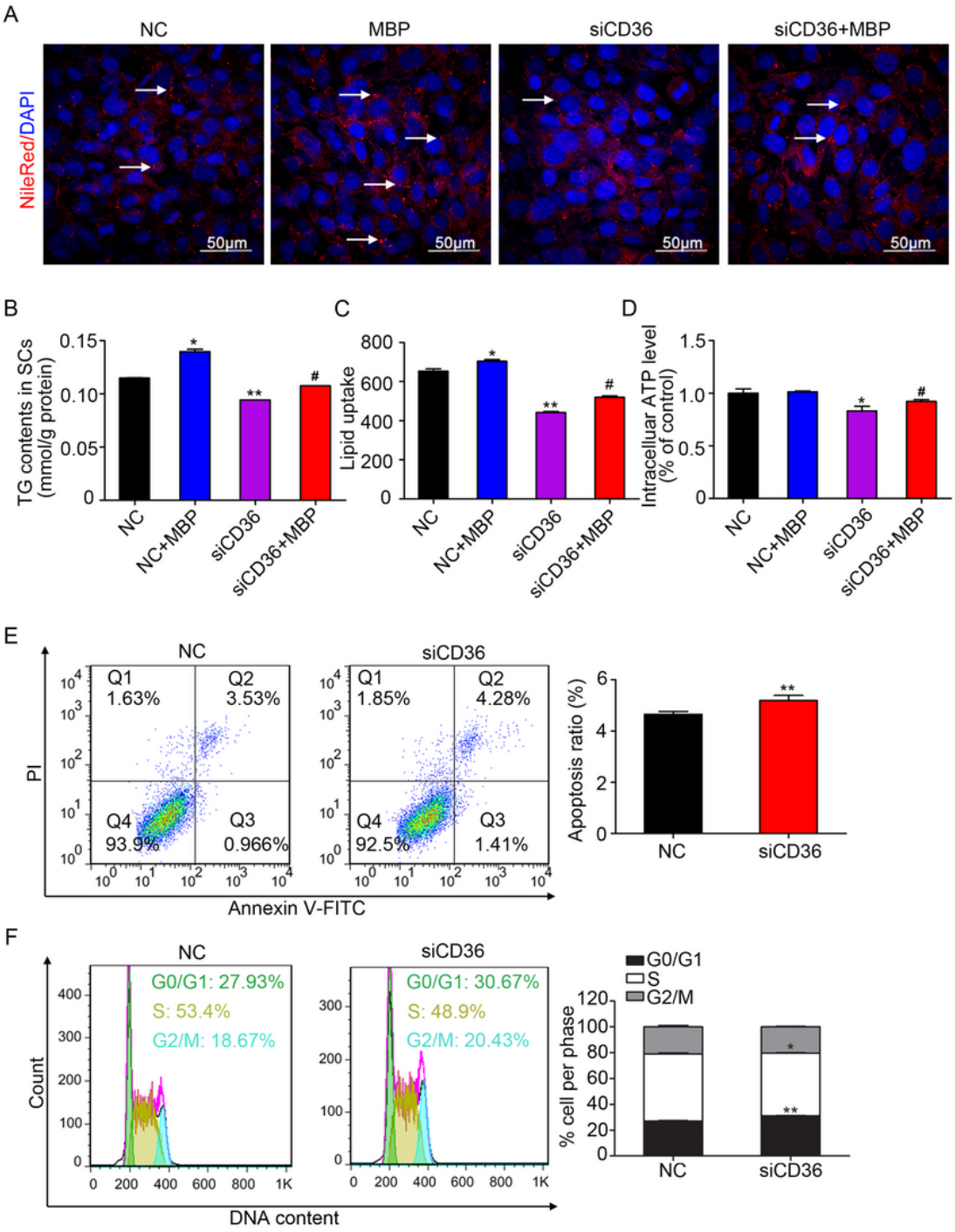

Figure 7

Effect of CD36 on FAs metabolism in TM4 cells. TM4 cells were transfected with control or CD36 knockdown plasmid and then treated with MBP. (A) Intracellular lipid content visualized with nile red (red) staining. Nuclei were stained with DAPI (blue). The arrow indicates lipid droplet. (B) TG levels were determined in cell lysates and expressed as millimoles TG/grams protein. (C) Bar graph depicting ELISA results of fatty acid uptake by TM4 cells using a Free Fatty Acid Uptake Assay Kit. (D) The intracellular

ATP content was performed using an ATP Assay Kit by a microbeta counter. (E) Apoptotic cells were stained with Annexin V-FITC/PI and analyzed by flow cytometry. The level of apoptosis in TM4 cells was calculated. (F) Cell cycle distribution was analyzed by flow cytometry. Results are expressed as means ± SEM (n = 3). ** $P < 0.01$; * $P < 0.05$, compared with the control. # $P < 0.05$, compared with MBP-treated group.

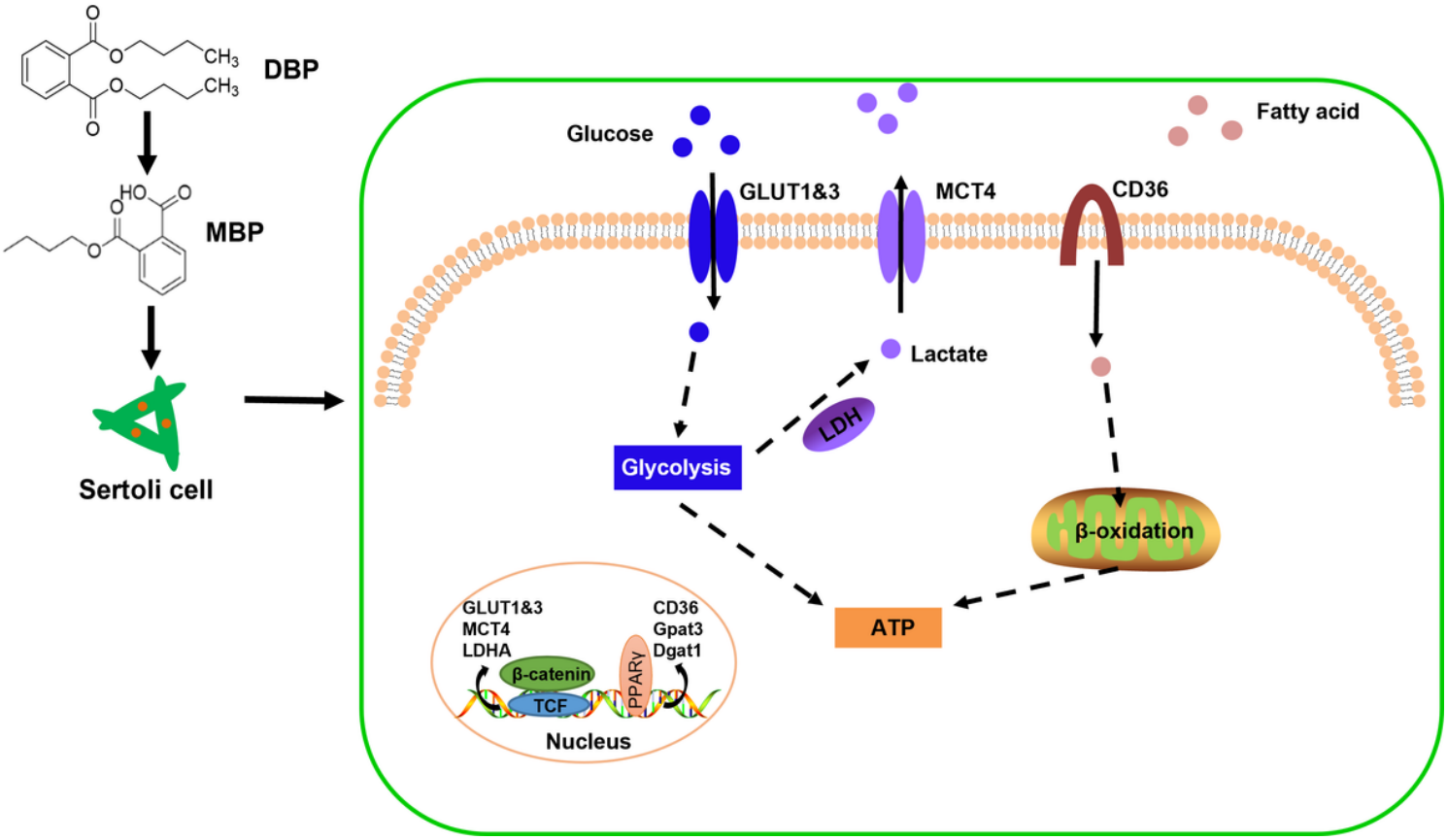

Figure 8

Legend not included with this version.

Supplementary Files

This is a list of supplementary files associated with this preprint. Click to download.

- Supplementary.docx